PROGRESSIVE BAYESIAN CALIBRATION OF THE BISON FUEL PERFORMANCE CAPABILITY

CHRISTOPHER MATTHEWS, GARRISON FLYNN, CETIN UNAL
Los Alamos National Laboratory
PO Box 1663, Los Alamos, NM – USA

ABSTRACT

Despite the fact that multiple computer codes have been developed, a robust predictive capability for quantifying fuel behavior and constituent distribution in metallic fuels and the associated uncertainty is still unavailable; large uncertainties and scatter still exist in predictions. Implementation of the statistical calibration approach over the previous manually adjusted coefficients has enabled rapid assessment of several thousand model evaluations that would have previously been impractical. Inclusion of expert judgment to the calibration process by weighting the error metric has been shown to accurately describe the phase transition temperatures and thermal conductivities. Furthermore, careful consideration in implementing the statistical approach provides a better understanding of standard variations in the model and presents a path forward for reducing model errors, such as missing dependence of porosity changes to the fuel's thermal conductivity model. Progressive calibration completed to date has supported the development of a more advanced, better-informed model calibration capability for improving the model's predictive accuracy.

1. Introduction

Model calibration is a systematic process by which predictions with variable parameters are compared with experiments to determine the optimal parameter set for model accuracy. Models are often calibrated with data available at specific experimental conditions, but utilized to predict in domains beyond feasible experiments. Establishing confidence in the applicability of these models to new domains requires analysis of model uncertainties and errors. To tackle these considerations, a progressive statistical approach to calibration was applied to the zirconium redistribution model within BISON. The model itself is summarized in [1]. Implementation of a statistical calibration approach enables rapid assessment of several thousand model evaluations. Information is added to the nominal calibration by inclusion of expert judgment by weighting experimental points based on importance, variability, and likely model form errors. A key benefit of statistical approach is the resulting posterior parameter and prediction distributions providing insight to uncertainties remaining in the model. Bayesian calibration forms these posterior distributions are probabilities of parameter values obtained by updating prior probabilities given insight from the evaluation of a large set of model samples. Resulting posteriors not only improve the model's predictive capability, but also provide guidance into potential future steps that may be taken to reduce model errors.

Calibration was applied to ternary metallic fuels. The primary data source for calibration was provided by zirconium atom fraction traces measured using electron probe microanalysis (EPMA) on irradiated fuel rods (See Fig. 1) during post irradiation examination (PIE). Two EPMA scans are available to calibrate against: T179 which was irradiated to ~2 a/o burnup [3], and DP16 which achieved burnups around 10 a/o [1].

Details of the experimental campaign, including irradiation cycle and rod parameters are provided in [5].

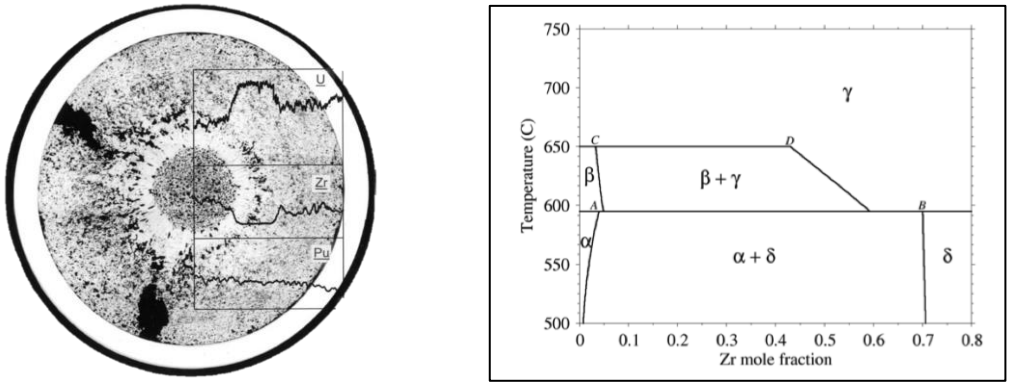

Fig 1: Typical irradiated U-Pu-Zr fuel rod with over-laid constituent concentration profiles, as well as the simplified phase diagram utilized during the calibration [1].

Calibration of the zirconium redistribution model focused on multipliers η applied to several of the parameters in the combined Soret and Fickian mass flux term formulated in [1]:

$$\mathbf{J}_{Zr} = - c_0 h_D D_0 \exp\left(\frac{- h_Q Q}{k_B T}\right)\left(\nabla x_{Zr} + x_{Zr}(1 - x_{Zr})\frac{h_{Q^*} Q^* + H}{RT^2}\nabla T\right)$$

The parameters utilized in the calibration are the three η parameters η_D, η_Q, and η_{Q^*}.Each of the calibration parameters and its associated material property are phase dependent, resulting in a four diffusional parameter calibration techniques for $\{\eta_D\}$, or 12 diffusional parameter calibration $\{\eta_D, \eta_Q, \eta_{Q^*}\}$. Also included in the calibration are the two horizontal temperature transitions A-B and C-D from the simplified phase diagram (Fig. 1) [1]. In the first stage of the study calibration was limited η_D and the A-B, C-D temperature transitions.

2. Model Calibration Framework

Let us represent a numerical model *M* such that the "true" values of parameter set **t** provides the best match to experimental measurements *y* at given control conditions, **x**. Experimental error ε is taken into consideration by stating that model predictions given the true model parameters are equal to measurements within the bounds of experimental error,

$$y(\mathbf{x}) = M(\mathbf{x}, \mathbf{t}) + \varepsilon(\mathbf{x}).$$

This formulation of a parameterized model assumes that governing physics of the system are perfectly represented. In reality, models are rarely exact replicas of reality, resulting in model form error *ψ*, causing even the true parameter set to produce bias predictions:

$$y(\mathbf{x}) = M(\mathbf{x}, \mathbf{t}) + \varepsilon(\mathbf{x}) + \psi(\mathbf{x}).$$

Model calibration may be employed when we do not know the true parameter values **t** or the model form error ψ. Bayesian calibration can provide distributions on the best fit values θ as well as estimate of model error, as proposed by Kennedy and O'Hagan [2] and implemented in a Bayesian context by Higdon et al [4]. Model form error in the traditional sense is neglected for the calibration presented herein, such that,

$$y(\mathbf{x}) = M(\mathbf{x}, q).$$

Rather than following traditional approaches of placing prior assumptions on the model error, prediction error for optimized parameters was analyzed, along with incorporation of expert opinion to provide suggestions of likely causes of error for future improvements of the BISON model. A progressive calibration was followed where more knowledge is incorporated to the model calibration step-by-step and new calibration parameters were also added to increase complexity and ideally, accuracy of predictions. Experimental error is not known for available data in this application and is therefore assumed negligible.

2.1 Traditional Model Calibration

Bayesian calibration samples parameter values from given prior distributions and evaluates the model to predict an outcome also measured experimentally. With each sample the model prediction is compared to the experimental measurement to calculate the prediction error, *e*. Nominal model error is represented as a vector of the absolute value of the difference between model predictions and experimental measurements at all available measurement points:

$$e(\mathbf{x}) = \left| M(\mathbf{x}, q) - y(\mathbf{x}) \right|.$$

In Bayesian calibration, if a new sample decreases the prediction error from a previous sample it is retained in the posterior distribution. Ultimately, model predictions should not be limited to a single fuel rod. Rather, the prediction vector can combine error for multiple cases into a single term (for example, combining predictions at T179 and DP16 irradiation conditions) resulting in simultaneous calibration of predictions across all test settings with a consistent parameter set. Errors across all settings and models are combined to a single, scalar error term by multiplying the error vector by the transpose of itself:

$$\text{Calibration Error} = e(\mathbf{x}) e(\mathbf{x})^T.$$

2.2 Expert-Weighted Model Calibration

There are cases in which an absolute best fit to experiments as achieved with the nominal error term is not ideal given model error and variability in measurements. For example, when a dataset exhibits large scatter in measurements from point to point, nominal calibration will attempt to fit to this scatter rather than determining the averaged best fit. Likewise predictions in some areas of the prediction may never be attainable due to missing physics in the model, however, nominal calibration may find the closest possible fit to such areas by sacrificing goodness of fit in others. The ‘black-box’ nature of traditional calibration causes such effects to reduce the overall quality of calibrated model predictions, particularly for extrapolation to new prediction domains.

We propose taking such factors into account by expert-opinion weighting of the error metric. The weighting term is a continuous variable from zero to one applied to each individual measurement:

$$e(\mathbf{x}) = w(\mathbf{x})\left| M(\mathbf{x},q) - y(\mathbf{x})\right|.$$

In general, higher weighting is given to experiments with low variability as well as experiments in important prediction regions such as the phase transition regions around the edges of the low zirconium concentration. Suspected model form error is also taken into account by applying a lower weighting to prediction regions that the model likely cannot replicate due to missing physics. The result of this weighting will hopefully result in more accurate predictions in important regions as well as avoidance of unphysical parameter compensations in regions where model-form error may dominate.

In addition to increasing efficiency of model calibration and introduction of expert opinion in an automated fashion, the statistical approach to model calibration provides a sense of remaining uncertainty, with respect to parameter values as well as resulting predictions.

3 U-Pu-Zr Parameter Optimization

As a first attempt at parameter calibration in previous work, visual best-fit calibration was applied to the phase dependent diffusivities in [1]. The next logical step was to apply the calibration framework described above to the same six parameters. In order to capture the subjectively determined regions of importance in the EPMA data, a weighted calibration technique was applied to “expert determined” weighting of the data sets. From there, the calibration parameters were increased from six to fourteen to further investigate the flexibility of the model without the implementation of new physics into the models. Lastly, new models were created through the use of the best available reactor operating data and full implementation of the metallic fuel models available in BISON.

All simulations except for the last run where the best available data was implemented, all runs were run as an axial fuel slice at the location of the EPMA cut. A daily-weighted power and fuel surface boundary condition were utilized. Except for a 10^5 second initial power ramp, the power and BC were held constant. Porosity was assumed constant, with thermal conductivity degradation factors qualitatively assigned to the porous central regions, dense β-phase ring, and semi-porous alpha regions. Refinement to the models with time dependent power, temperature, and porosity, was implemented in the “refined input” calibration.

For the last run, the temperature boundary condition and pin powers were utilized in a full 2D-Rz BISON simulation with the best available models but without zirconium redistribution. The temperature BC and axial fission rates were extracted and utilized in an axial fuel slide at the location of the EPMA cut. This ensured errors due to pin power and temperatures were reduced to the best available operational data.

3.1 Six Parameter Calibration

Six parameters were first considered in the original U-Pu-Zr model. Since the parameter set is assumed to represent the fuel throughout the entire lifetime the same parameter values should be used to predict both T179 (~2% burnup) and DP16 (~10% burnup). However, model errors, such as neglecting changing porosity in the model, can cause

the model to calibrate to different parameter values at the different burnup values. Accuracy of the model was tested by first optimizing parameters using T179 data alone and DP16 data alone.

Five thousand simulations are completed to explore the parameter space. Parameters were given a uniform distribution with bounds provided in Table 1, with the condition that the A-B transition temperature must always be at least 20 K lower than the C-D temperature.

The single best simulation results for independently calibrated cases are shown in Fig. 2. Predictions with the T179 optimized parameters appear to be fitting to the scatter of data in the outer phase transition, drawing the low Zr β-phase region to higher Zr atom fraction than observed in experiments. DP16 optimized parameters predict the inner and outer phase transitions accurately, but are unable to capture the subtle transition in the bathtub region, instead preferring a sharp drop off to a low Zr atom fraction around the 0.75 mm radius.

Optimized parameters for the individual cases are then applied for predicting the case held out from calibration. For example, parameters optimized for T179 simulations are implemented for prediction of DP16 data. If no model form error were present, the extrapolated predictions would be expected to adequately predict DP16. Clearly such accuracy is not achieved, as illustrated in Fig. 2. Most notably T179 parameters are unable to predict the DP16 data set, particularly at the inner phase transition. In addition, DP16 parameters over-predict the inner phase transition of T179 while under-predicting the outer phase transition.

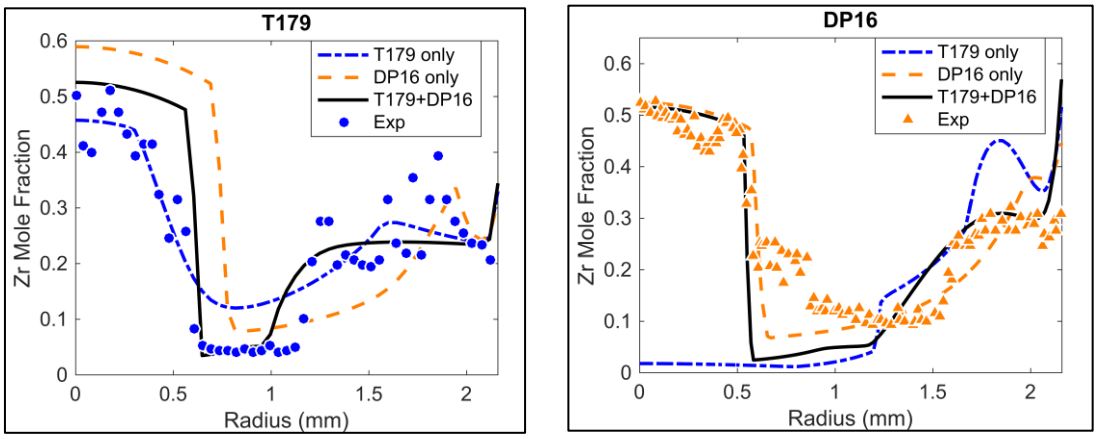

Fig 2. Zirconium concentration profiles using the optimized six-parameter calibration coefficients.

Ideally, the applied calibration technique would determine parameter values that provide the best predictions at the most important regions of the distribution curve and mitigate fit to scatter in the data by calibrating with the expert-opinion weighted error metric. Weights applied to the U-Pu-Zr cases are shown in Fig. 3. The depleted Zr region of T179 is selected as important (w=1) because the data set has less scatter in this region and is more representative of an out-of-pile phase diagram, as opposed to the high burnup DP16 data where the fission products may have influence over the thermodynamics of the system. The outer phase transition and center region of DP16 is

also given high importance because of the lower scatter in data. The T179 outer phase transition and center region with large scatter are weighted at *w*=0.5. Due to the simplistic phase diagram, the shelf of the DP16 bathtub will likely be unachievable with the current model form, thus this region is weighted low at *w*=0.2 to avoid parameter compensations in other regions.

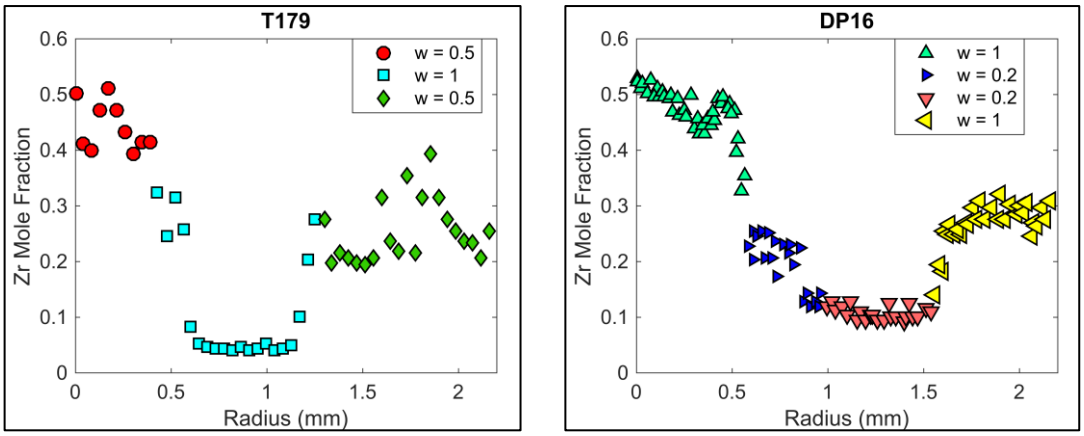

Fig 3. Weights applied to the data sets.

Resulting model predictions with expert-weighted calibrated parameter values are shown in Fig. 4 while Fig. 5 shows the mean prediction for both cases when with the combined parameter posteriors as well as the accompanying uncertainty bounds.
Most notable, the outer radius (>1.5 mm) with *w=1* shows significant improvement in fit from the unweighted case while the inner radius, also *w=1*, shows lower average predictions. The significance of this finding is that by lowering the weight on the depleted Zr region, which we know can never be accurately predicted due to missing physics; we are able to improve the predictive capability in the regions more adequately modeled.

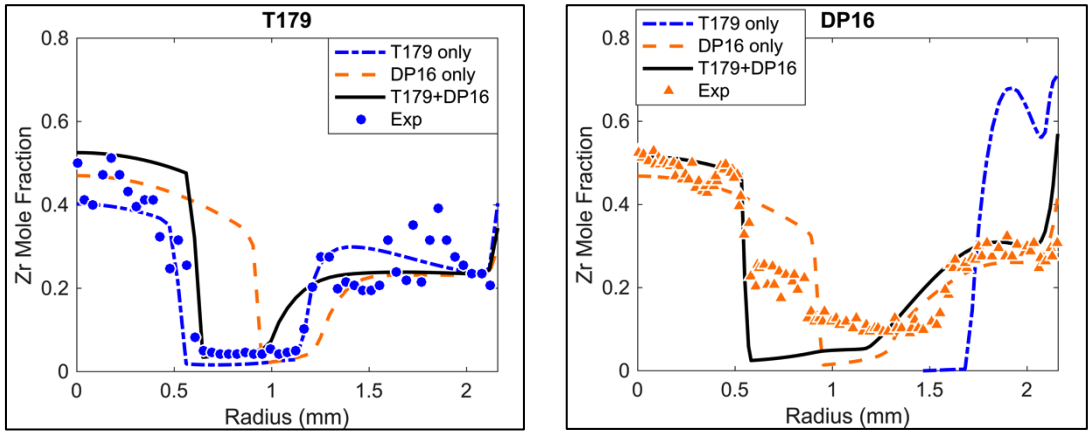

Fig 4. Zirconium concentration profiles using the optimized weighted six-parameter calibration coefficients.

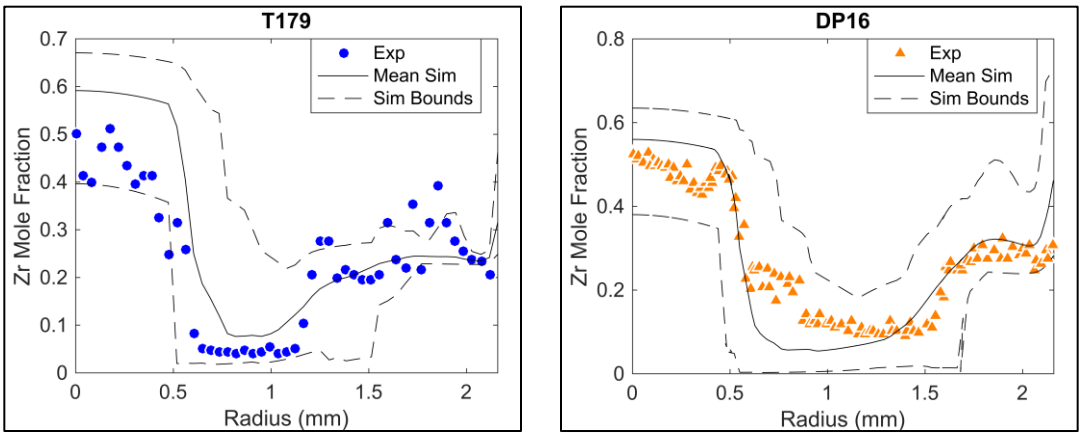

Fig 5. Upper and lower boundaries of optimized predictions using weighted posterior parameter distributions.

Table 1 compares the posterior parameter distributions of the nominal and weighted calibration to the prior distributions. Evaluating the standard deviation of the posterior distributions gives an indication the sensitivity of the model to each parameter. Diffusion coefficient for the β-phase, $\eta_{D,\beta}$, is found to have the largest standard deviation in the posterior indicating that it is not able to be calibrated well due to having little effect on predictions. Diffusion coefficient for the γ-phase, $\eta_{D,\gamma}$ has the lowest standard deviation and therefore appears most influential. A likely cause of the tight posterior distribution for $\eta_{D,\gamma}$ is the model's inability to converge to a solution at higher $\eta_{D,\gamma}$ values. Recall from Fig. 2 that the combined calibration considering T179 and DP16 simultaneously produced the best compromise of results predicting both cases. Values shown in Table 1 are for combined calibration.

Parameter	Prior Distribution		Nominal Calibration		Expert-Weighted Calibration	
	Min	Max	Mean	Std	Mean	Std
$\eta_{D,\alpha}$	0.01	100	17.3	14.1	17.3	13.2
$\eta_{D,\beta}$	0.01	20	51.4	30.9	50.8	30.8
$\eta_{D,\gamma}$	0.01	100	16.3	11.3	19.8	11.8
$\eta_{D,\delta}$	0.01	100	0.93	0.69	0.92	0.69
A-B [K]	850	1100	943	34.7	947	29.7
C-D [K]	900	1150	1013	25.1	1016	24.0

Tab 1: Summary of posterior distribution statistics for six parameter U-Pu-Zr model calibration.

3.3 Fourteen Parameter Calibration

Next, the number of uncertain parameters in the model is increased with the goal of narrowing down specific components of the governing behavior affecting predictions. Along with the multiplier against diffusivity pre-exponential, the multipliers against the activation energy η_Q and heat of transport η_{Q^*} for each of the four phases is included to bring the total number of calibration parameters to 14.

Once again, parameters are optimized for the individual cases first and predictions are extrapolated to the hold out case. Resulting predictions are shown in Fig. 6 where improvements for T179 and DP16 due to the independently calibrated cases are clear. T179 appears to have less reaction to scatter in the data with a smoother fit through the averaged zirconium atomic fraction. DP16 predictions are drastically improved, with the increased model flexibility allowing a match to measurements throughout the entire radius.

Extrapolation of parameters to from one case to another, however, is still found to produce large prediction errors indicating missing physics in the model. Behavior of DP16 predictions with the T179 parameters is similar to the six-parameter model and fails to predict the correct zirconium atomic fraction in any region of the rod and T179 predictions with the DP16 model parameter over-predicting the bathtub.

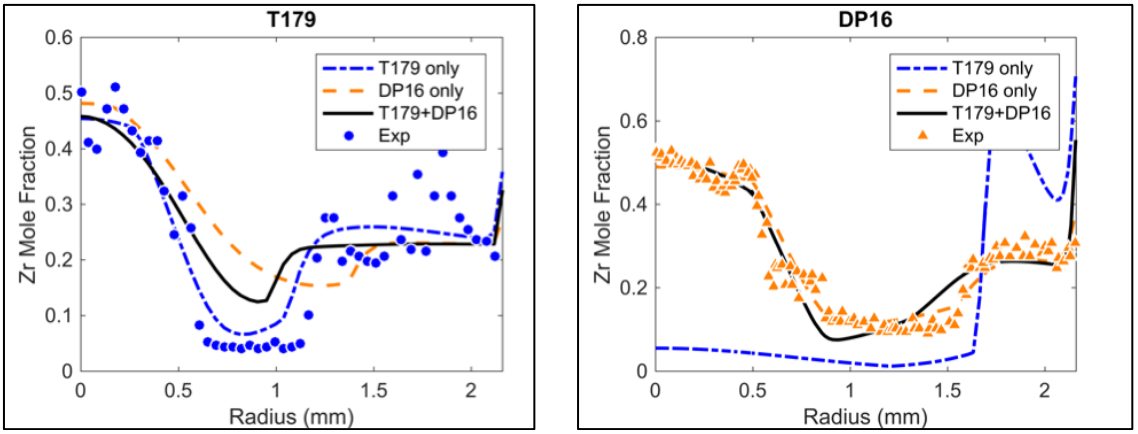

Fig 6. Zirconium concentration profiles using the optimized weighted 14-parameter calibration coefficients.

Parameters are then calibrated considering T179 and DP16 simultaneously to find the averaged, best fit parameters across both cases. Statistics of calibrated posteriors are provided in Table 2. Combined calibration tends to favor DP16 independently calibrated parameter values. The $\eta_{D,\alpha}$, $\eta_{D,\beta}$, and $\eta_{D,\delta}$ coefficients as well as A-B transition temperature have notable change in value from T179 calibration to DP16 calibration.

Parameter	Prior Distribution		Expert-Weighted Calibration	
	Min	Max	Mean	Std
$\eta_{D,\alpha}$	0.1	10	4.20	2.85
$\eta_{D,\beta}$	0.1	100	47.2	27.13
$\eta_{D,\delta}$	0.1	10	2.85	2.92
$\eta_{D,\gamma}$	0.1	1	0.66	0.23
$\eta_{Q,\alpha}$	0.9	1.1	1.03	0.05
$\eta_{Q,\delta}$	0.9	1.1	1.05	0.04
$\eta_{Q,\beta}$	0.9	1.1	1.04	0.04
$\eta_{Q,\gamma}$	0.9	1.1	0.97	0.05
$\eta_{Q^*\alpha}$	0.5	2	1.13	0.45
$\eta_{Q^*\delta}$	0.5	2	1.19	0.57
$\eta_{Q^*\beta}$	0.5	2	1.27	0.14
$\eta_{Q^*\gamma}$	0.5	2	1.48	0.95
A-B [K]	850	950	934	12.4
C-D [K]	900	1000	986	9.5

Tab 2: Summary of posterior distribution statistics for fourteen parameter U-Pu-Zr model calibration.

3.4 Refined Input

Following expansion of the number of parameters the model can be calibrated against, an alternate pathway towards achieving favorable calibration results was tested by applying the calibration process to BISON runs that utilized the best available data and models. By taking away as much uncertainty as possible associated with the reactor cycle data, rod fabrication data, and BISON implementation, the calibration may provide insight into if the underlying BISON model is adequate to provide the necessary baseline simulation capabilities.

The refined input models were created by initially starting with simulations of the full reactor pins. The experimental data was utilized to try and capture the reactor operating conditions as close as possible to the environment the pins were subjected to. Utilizing the cut height of samples used for the EPMA scans, a fuel surface temperature profile as a function of temperature was extracted from the full pin simulations and applied as a boundary condition to one dimensional calibration models. In addition, the currently implemented fission gas swelling model in BISON was utilized to provide a porosity degradation term to the thermal conductivity of the model. As discussed in [4], the model is an oversimplification of the actual swelling behavior, and is targeted for replacement.

The refined input cases were run with similar prior parameter distributions as the six parameters calibration and weight functions shown in Fig. 3. Best case predictions with the independently and simultaneously calibrated parameters are compared in Fig. 7. The refined model is found to provide better overall predictions for both T179 and DP16, particularly at the inner phase transition of T179 and outer transition of DP16. However, extrapolating individual case calibrated parameters is still found to be insufficient indicating remaining model form error exists. In fact, when the DP16 model is run with T179 best case parameters the simulation is not able to converge, thus no predictions with T179 parameters can be compared.

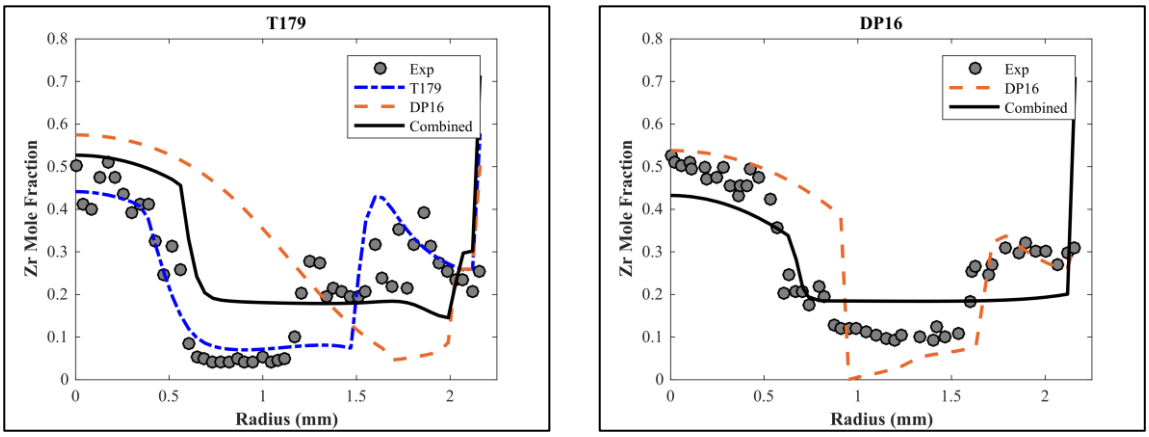

Fig 7. Zirconium concentration profiles using the optimized weighted six-parameter calibration coefficients with refined model inputs.

Model parameters were also calibrated using T179 and DP16 simultaneously, again using the expert-opinion weighting function. Predictions given the combined calibration continue to encompass the majority of T179 data, but begin to under predict the DP16 outer phase transition. Once again, results shed light on likely model form errors making prediction of both T179 and DP16 cases unreasonable with a single set of model parameters. Compared to prior uncertainty the feasible range from $\eta_{D,\alpha}$, $\eta_{D,\gamma}$ and $\eta_{D,\delta}$ is clearly reduced, while the $\eta_{D,\beta}$ remains highly uncertain and therefore likely uninfluential. A bimodal trend is beginning to form in the C-D transition temperature, indicating the high transition temperature needed to predict T179 accurately in contrast with the low transition temperature needed to predict DP16 accurately.

	Nominal		Expert-opinion Weighted		14-parameter		Refined Input	
	Mean	Std	Mean	Std	Mean	Std	Mean	Std
T179	0.078	0.007	-	-	0.074	0.004	0.159	0.052
DP16	0.101	0.012	-	-	0.054	0.004	0.139	0.044
Combined	0.118	0.010	0.094	0.011	0.070	0.003	0.195	0.045

Tab 3: Root mean square error mean and standard deviations for the different calibration techniques.

5 Summary and Conclusions

Calibration of the original U-Pu-Zr BISON model along with investigation into parameter and prediction tradeoffs revealed model form error. When calibrated to either T179 or DP16 independently, parameters do not extrapolate accurate predictions on the other rod indicating a lack of physical accuracy in the model. Although consideration of both rods simultaneously allows for a calibrated parameter set to be found that reduced uncertainty in predictions across both rods, the indication of missing physics remains concerning. Keeping this error in mind, qualitative weighting was applied to inform the calibration of regions less likely to match experiments due to missing physics. This expert-weighted calibration was found to improve the predictive capability. It is likely that

applying lower weighting at areas with known model discrepancy helped to prevent unphysical compensation between parameters.

The fourteen parameter model, while providing more flexibility in the zirconium distribution across the radius for DP16, is not found to be a significant improvement over the six parameter model in terms of extrapolation accuracy. The refined model is found to improve predictions and result in reasonable prediction bounds. Discrepancy in calibrated parameters between the two cases remains, indicating a missing dependency in the model for which parameters should be reliant. This tradeoff maintains the prior conclusion that model form error exists and is prohibitive to matching both data sets.

[1] GALLOWAY, J., UNAL, C., CARLSON, N., PORTER, D., HAYES, S., Modeling constituent redistribution in U–Pu–Zr metallic fuel using the advanced fuel performance code BISON, Nuclear Engineering and Design **286** (2015) 1.

[2] KENNEDY, M.C., O'HAGAN, A., Bayesian calibration of computer models, J Royal Statistical Soc B **63** 3 (2001) 425.

[3] KIM, Y.S., HOFMAN, G.L., HAYES, S.L., SOHN, Y.H., Constituent Redistribution in U-Pu-Zr Fuel During Irradiation, Journal of Nuclear Materials **327** 1 (2004) 27.

[4] HIGDON, D., GATTIKER, J., WILLIAMS, B., RIGHTLEY, M., Computer Model Calibration Using High-Dimensional Output, Journal of the American Statistical Association **103** 482 (2008) 570.

[5] MATTHEWS, C., STEVENS, G., GALLOWAY, J., WILKERSON, R.B., UNAL, C., Assessment of the Coupled Thermal-Mechanical-Diffusion Models in BISON for Metallic Fuel Constituent Redistribution, LA-UR-17-28763, (2017) 1.